J. Chosun Natural Sci.
Vol. 9, No. 4 (2016) pp. 241 – 248
https://doi.org/10.13160/ricns.2016.9.4.241

Comparative Molecular Similarity Indices Analysis (CoMSIA) of 8-substituted-2-aryl-5-alkylaminoquinolines as Corticotropin-releasing factor-1 Receptor Antagonists

Santhosh Kumar Nagarajan[1] and Thirumurthy Madhavan[1,2†]

Abstract

Corticotropin-releasing factor receptors (CRFRs) activate the hypothalamic-pituitary-adrenal axis, which is an integral part of the fight or flight response to stress. Increase in CRH level is observed in Alzheimer's disease and major depression and hypoglycemia. Here, we report on the relevant physicochemical parameters required for the CRFR inhibitors. Comparative molecular similarity indices analysis (CoMSIA) was performed with the derivatives of 8-substituted-2-aryl-5-alkylaminoquinolinesas CRFR inhibitors. The best predictions were obtained for the best CoMSIA model with a q^2 of 0.576 with 6 components and r^2 of 0.977. The statistical parameters from the generated CoMSIA models indicated that the data are well fitted and have high predictive ability. CoMSIA contour maps could be useful in the designing of more potent and novel CRFR derivatives.

Keywords: 3D-QSAR, CoMSIA, CRFR, CRHR

1. Introduction

Corticotropin - releasing hormone (CRH) is a 41 amino acid peptide hormone[1]. It is also known as also known as corticotropin - releasing factor (CRF). It is involved in the stress response as a neurotransmitter, which is secreted in the paraventricular nucleus (PVN) of the hypothalamus. It is also found in the peripheral tissues, such as T lymphocytes, and is highly expressed in the placenta[1]. Their function is mediated by a family of receptors called Corticotropin -releasing factor receptors (CRFRs). They are G protein-coupled receptors, which have seven transmembrane helices[2]. There are two types of CRFR receptors, type 1 and 2, which are encoded by separate genes (CRHR1 and CRHR2 respectively)[3]. CRF1 receptor is involved in the regulation of ACTH, which is an important mediator of the stress response. It is abundant in the pituitary.

[1]Department of Bioinformatics, School of Bioengineering, SRM University, SRM Nagar, Kattankulathur, Chennai 603203, India.
[2]Department of Genetic Engineering, School of Bioengineering, SRM University, SRM Nagar, Kattankulathur, Chennai 603203, India.

†Corresponding author : thiru.murthyunom@gmail.com, thirumurthy.m@ktr.srmuniv.ac.in
(Received : October 17, 2016, Revised : December 17, 2016, Accepted : December 25, 2016)

Corticotropin Releasing-Hormone (CRH) activates the hypothalamic-pituitary-adrenal axis (HPA axis), which is one of the two parts of the fight or flight response to stress[4]. An increase in the level of CRH has been observed to be associated with Alzheimer's disease and major depression[5], and autosomal recessive hypothalamic corticotropin deficiency fatal metabolic consequences including hypoglycemia[1]. Chronic activation of CRHR1s by CRH, induced by early life stress, might result in memory deficits and learning impairments and anxiety in adulthood.

CRF present in the Central nervous system (CNS) has been linked to a variety of disorders including depression, stress, anxiety, post-traumatic stress disorder, and addiction. CRF has been shown to be involved in the stress-induced phosphorylation of tau which implies a potential link between stress and Alzheimer's disease pathology[6]. It is also present in the periphery where it is involved in inflammation, and cancer. CRF may be one of the links between stress and cancer. Also, a recent research suggested that CRF plays a major role in the development and maintenance of bone cancer pain via activation of neurons.

Several research groups have indulged on the discovery of CRF1 receptor antagonists for the treatment of

depression or other stress-related disorders. However, the benefits of blocking the CRF2 receptor remain uncertain. Pexacerfont, Antalarmin, CP-316311 and CP-154,526 are the available antagonists for CRF1. Pexacerfont, a recently developed CRF-1 antagonist, is currently in clinical trials for the treatment of anxiety disorders[7]. Antalarmin are used in the animal trials for the treatment of anxiety, depression and other conditions, but no human trials have been carried out. Also, the results have had limited success so far, and they have failed to produce an effect comparable with conventional antidepressant drugs[8]. The drug CP-316311 was unsuccessful in a double-blind study for depression[9]. CP-154,526 is under investigation for the potential treatment of alcoholism[10]. Hence, it is apparent that the discovery of structurally diverse CRF1 receptor antagonists and the accumulation of clinical studies for clarifying the role of CRF in humans are essential.

2. Computational Methods

2.1. Dataset

From a literature, which reported 8-substituted-2-aryl-5-alkylaminoquinolines derivatives as the inhibitors for CRF1 receptor[11], 23 compounds with their biological activities were taken. IC_{50} values of each inhibitor was converted into pIC_{50} ($-\log IC_{50}$) in order to use the data as dependent variable in CoMSIA model. The test set molecules were selected which is the representative molecule for training set molecules. The test set molecules were selected manually so as to cover all the biological activity which is similar to the training set molecule. The total set of compounds was divided into a training set consist of 16 compounds and test set consist of 7 compounds. The structures and their activity values are displayed in Table 1.

Table 1. Structures and biological activities (pIC_{50}) of CRFR inhibitors

The indole/azaindole CRFR inhibitor scaffold

a) Compound 1-8

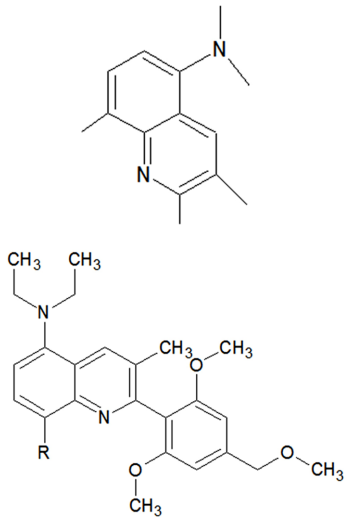

Compound	R	pIC50 values
1	Methyl	7.102
2	F	6.646
3	Cl	7.208
4	CF_2H	6.383
5	CF_3	6.541
6	CN	6.991
7	Methoxymethyl	6.000
8	OMe	6.959

Table 1. Continued

b) Compound 9-15

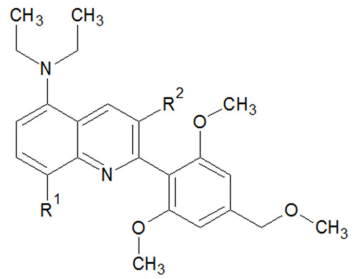

Compound	R^1	R^2	pIC50 values
9	OMe	H	6.695
10	OMe	F	6.928
11	OMe	Cl	6.842
12	OMe	Ethyl	6.967
13	Me	H	6.735
14	Me	F	6.842
15	Me	Cl	7.091

c) Compound 16-20

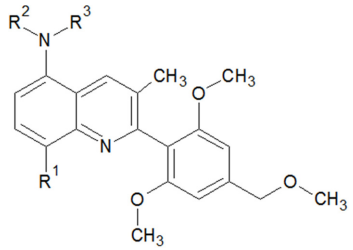

Compound	R^1	R^2	R^3	pIC50 values
16	OMe	nPr	nPr	6.979
17	OMe	Ethyl	Methoxyethyl	6.407
18	OMe	Isobutyl	Methoxyethyl	6.807
19	Me	nPr	nPr	7.055
20	Me	Ethyl	Methoxyethyl	6.963

d) Compound 21-23

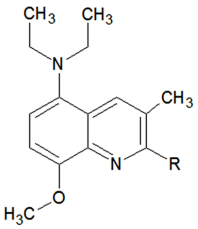

Compound	R^1	pIC50 values
21	2-chloro-4-methoxymethyl-6-methoxyphenyl	7.174
22	2,6-dimethoxy-4-cyanophenyl	6.880
23	2,6-dimethoxy-4-methylphenyl	7.004

2.2. Ligand-Based Alignment Method

For each compound, the partial atomic charges were assigned by utilizing Gasteiger-Hückel method available in SYBYLX 2.1 package (Tripos Inc., St. Louis, MO, USA). All rotatable bonds were searched with the incremental dihedral angle from 120° by using systematic search conformation method. Conformational energies were computed with the electrostatic term, and the lowest energy conformer was selected as the template molecule. Then the template was modified for other ligands of the series. The common scaffold was a constraint for each molecule, and only the varying parts were energy minimized by Tripos force field with Gasteiger-Huckel charge by using conjugate gradient method, and convergence criterion was 0.05 kcal/mol at 10,000 iterations. The minimized structures were aligned over the template using the atom fit method, and subsequently, this alignment is used for CoMSIA. The aligned molecules are represented in Fig. 1.

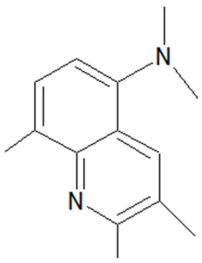

(a)

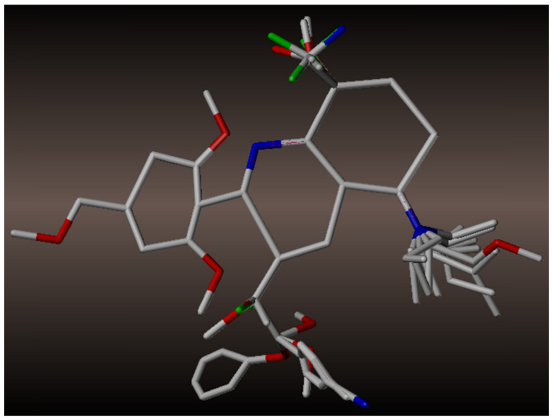

(b)

Fig. 1. (a) Maximum common substructure present in all molecules. (b) Alignment of molecules based on systematic search conformation of highly active compound 8.

2.3. CoMSIA Field Generation

SYBYLX 2.1 (Tripos Inc., St. Louis, MO, USA) package molecular modeling package was used for the 3D QSAR studies based on CoMSIA. Steric, electrostatic, hydrophobic, H-bond acceptor and donor fields were used for this study. CoMSIA studies help in deriving a relation between the biological activities and three-dimensional structures of the set of molecules of the dataset. The molecular alignment was placed in a 3D grid, and the molecular field values of each conformation of a molecule are calculated. 2 Å lattice spacing was used. The CoMSIA method was performed using steric and electrostatic fields with standard ±30 kcal/mol cutoffs. CoMSIA calculated steric and electrostatic field values.

2.4. Partial Least Square (PLS) Analysis

PLS algorithm quantifies the relationship between the structural parameters and the biological activities[12,13]. CoMSIA descriptors used as independent variables and pIC_{50} values used as dependent variables in PLS analysis for the generation of 3D-QSAR models. Leave-one-out (LOO) cross-validation procedures were used to obtain the cross-validated correlation coefficient (q2), non-cross-validated correlation coefficient (r2), standard error estimate (SEE) and Fisher's values (F)[14,15]. A non-cross-validated analysis was carried out without column filtering was then followed. The cross-validated correlation coefficient (q^2) was calculated using the following equation:

$$q^2 = 1 - \frac{\sum_{\gamma}(\gamma_{pred} - \gamma_{actual})^2}{\sum_{\gamma}(\gamma_{actual} - \gamma_{mean})^2}$$

where γ_{pred}, γ_{actual}, and γ_{mean} are the predicted, actual, and mean values of the target property (pIC_{50}), respectively.

The predictive power of CoMSIA models was determined from the set of seven test molecules which was excluded during model development. The predictive correlation coefficient (r^2_{pred}) based on the test set molecules, is defined as:

$$r^2_{pred} = \frac{(SD - PRESS)}{SD}$$

where PRESS is the sum of the squared deviation between the predicted and actual activity of the test set

molecules, and SD is defined as the sum of the square deviation between the biological activity of the test set compounds and the mean activity of the training set molecules.

3. Results and Discussion

3.1. CoMSIA Analysis

A reliable CoMSIA model was derived with the combination of the different field contributions and Gasteiger-Hückel charge method with 2.0 Å grid space. Various combinations of training and test compounds were used for model generation. Many CoMSIA models were obtained, of those only five models was selected based on the reliable q^2 and r^2_{pred} values. The statistical values of the five models are tabulated in Table 2. The Leave one out (LOO) analysis gave the cross-validated q^2 of 0.576 with 6 components and non-cross-validated PLS analysis resulted in a correlation coefficient r^2 of 0.977, Fisher value as 69.440, and an estimated standard error of 0.063. The predictive ability of the developed CoMSIA model was assessed by the test set (6 molecules) predictions, which were excluded during model generation. The predictive ability of the test set was 0.603. Predicted and experimental activities and their residual values of all inhibitors are shown in Table 3, and the corresponding scatter plot is depicted in Fig. 2.

3.2. CoMSIA Contour Map

Color-coded contour maps were generated using CoMSIA analyses which represent regions in 3D space where changes in the different fields of a compound correlate strongly with changes in its biological activity. A scalar product of coefficients and standard deviation (SD*Coeff) associated with each column were generated as contour maps. Favored levels were fixed at 70% and disfavored levels were fixed at 30%.

The CoMSIA contour map was generated based on the ligand-based (atom-by-atom matching) alignment method. The CoMSIA result is represented as a 3D 'coefficient contour' map. The steric contour map is displayed in Fig. 3. The green color contour maps depict the bulk molecules favored region whether yel-

Table 2. Statistical results of CoMSIA models obtained from systematic search conformation based alignment

PLS statistics	Ligand-based CoMSIA model (Systematic search conformation based alignment)				
	Model 1	Model 2	Model 3	Model 4	Model 5
q^2	0.576	0.566	0.530	0.506	0.490
N	6	6	6	6	6
r^2	0.977	0.977	0.970	0.970	0.971
SEE	0.063	0.060	0.070	0.071	0.064
F-value	69.440	71.217	54.456	54.602	55.281
r^2_{pred}	0.603	0.512	0.501	0.454	0.432
	Field contribution				
Steric	0.089	0.085	0.087	0.089	0.085
Electro static	0.333	0.334	0.334	0.308	0.375
Hydrophobic	0.401	0.417	0.395	0.412	0.403
Donor	0.000	0.000	0.000	0.000	0.000
Acceptor	0.177	0.164	0.185	0.191	0.137

q^2= cross-validated correlation coefficient; N= number of statistical components; r^2= non-cross validated correlation coefficient; SEE=standard estimated error; F=Fisher value; $r^2_{predictive}$= predictive correlation coefficient for test set.

The model chosen for analysis is highlighted in bold fonts.

Test set compounds

Model 1- compound no 2, 6, 8, 12, 20, 22
Model 2- compound no 2, 6, 8, 12, 20, 21
Model 3- compound no 2, 6, 8, 12, 20, 23
Model 4- compound no 2, 6, 8, 10, 20, 22
Model 5- compound no 2, 6, 8, 17, 20, 21

Table 3. Predicted activities and experimental pIC_{50} values obtained from CoMSIA models

Compound	Actual pIC_{50}	Predicted	Residual
1	7.102	7.097	0.005
2*	6.928	6.860	0.068
3	6.842	6.935	-0.093
4	6.967	6.722	0.245
5	6.735	6.741	-0.006
6*	6.842	6.903	-0.061
7	7.091	6.978	0.113
8*	6.979	6.973	0.006
9	6.407	6.430	-0.023
10	6.807	6.786	0.021
11	7.055	7.065	-0.01
12*	6.646	6.517	0.129
13	6.963	6.535	0.428
14	7.174	7.214	-0.04
15	6.879	6.922	-0.043
16	7.004	6.963	0.041
17	7.208	7.227	-0.019
18	6.383	6.429	-0.046
19	6.541	6.490	0.051
20*	6.991	7.032	-0.041
21	6.000	6.003	-0.003
22*	6.959	6.726	0.233
23	6.695	6.698	-0.003

*Test set compounds

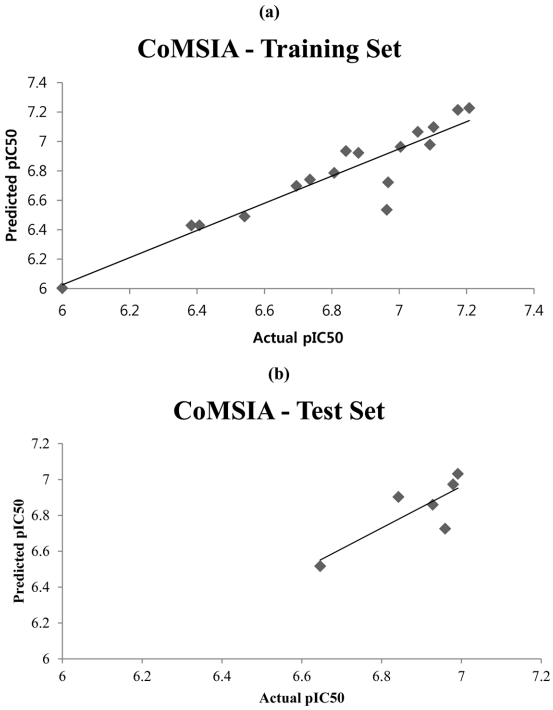

Fig. 2. (a and b) Plot of actual versus predicted pIC50 values for the training set and test set for the CoMSIA values performed after atom-by-atom matching alignment by systematic search

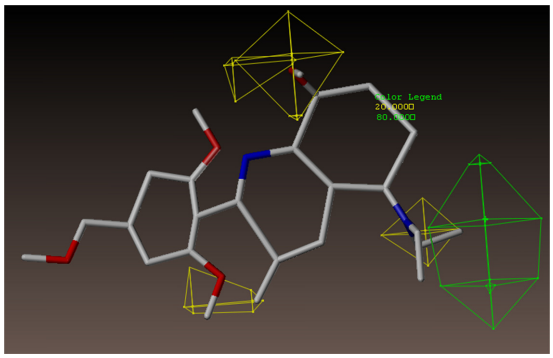

Fig. 3. CoMSIA steric contour map with highly active compound 8 for systematic search based alignment. Here green contour indicates the region where large group increases activity, and yellow contours indicate large group decreases activity.

low color region represents the area where the bulk molecules not favored. A green contour region is seen near the R_1 position of the phenyl ring. It denotes that a bulky group substitution required at this position for high activity. Compounds 1, 6 and 8 with a bulkier substituent at this position are more active, which represent the importance of bulky substitution at the position. A yellow contour region was seen near the green contour map in R position; the contour map clearly indicated that substitution of bulkier groups would decrease the activity, which might be the reason for the low activity of compounds 4, 5 and 7 having a bulkier substitution.

The electrostatic contour map is represented in Fig. 4. In the case of the electrostatic field contours, red regions represent electronegative substituents favored regions, and blue regions represent electropositive substituents favored regions. The electrostatic contour plot shows that there is a blue colored region situated close to the R positions. It indicates that the electropositive charges in these areas are crucial for ligand binding, and an electropositive group linked to this position will enhance the biological activity.

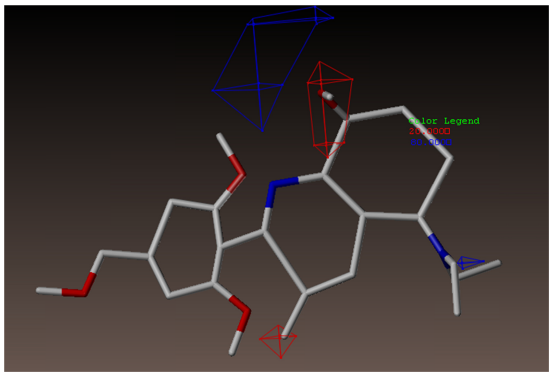

Fig. 4. CoMSIA electrostatic contour map with highly active compound 8 for systematic search based alignment. Here blue contour indicates regions where electropositive groups increase activity, and red contours indicate areas where electronegative groups increase activity.

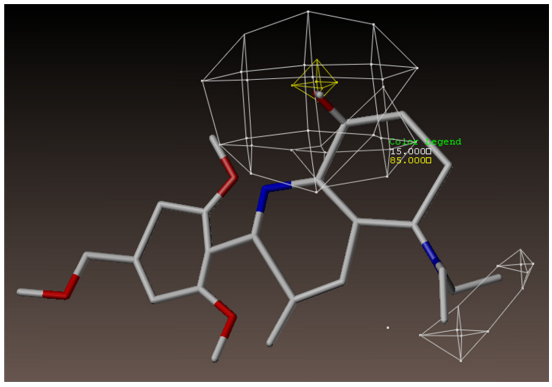

Fig. 5. CoMSIA hydrophobic contour map with highly active compound 8 for Systematic search based alignment. Yellow contour map indicates the region where the hydrophobic substitutions are favorable for activity, and white contour indicates the disfavoured region for inhibitory activity

Hydrophobic contours are represented in Fig. 5, where the yellow regions indicate the area where the hydrophobic substitutions are favorable for activity, and white contour indicates the disfavoured region for inhibitory activity. A big white contour is seen around the R substitution position, where the hydrophobic substitutions are not favorable. Compound 20 well account for this phenomenon, which has low activity because of the hydrophobic substitution at the position.

CoMSIA H-bond acceptor contour map with highly active compound 8 is represented in Fig. 6. Here,

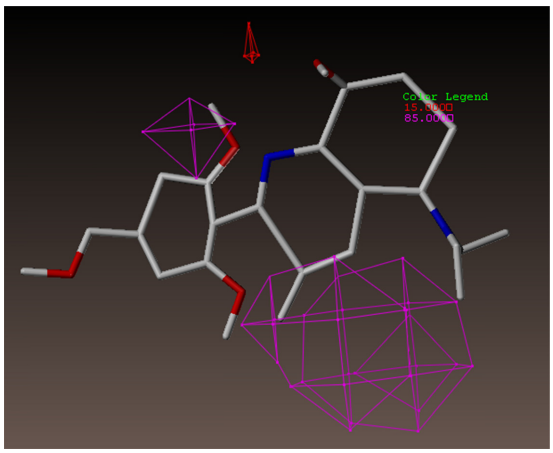

Fig. 6. CoMSIA H-bond acceptor contour map with highly active compound 8 for systematic search based alignment. In H-bond acceptor field contour, magenta contour map indicates where hydrogen bond acceptor group increases the activity and red contour map indicates the hydrogen bond acceptor group decreases the activity.

magenta contour map indicates where hydrogen bond acceptor group increases the activity and red contour map indicates the hydrogen bond acceptor group decreases the activity. CoMSIA H-bond donor contour map is not represented as their field contribution was zero. The results from the CoMSIA contour maps were consistent with the CoMFA contour maps, which we performed earlier[16].

4. Conclusion

In this study, a satisfactory CoMSIA model from 8-substituted-2-aryl-5-alkylaminoquinolines derivatives as Corticotropin-releasing factor-1 receptor antagonists was developed based on atom-by-atom matching alignment. The contour map indicated important sites, such as steric, electrostatic, hydrophobic and H-bond acceptor could influence the biological activities of the compounds. The results obtained from this study have thrown light on the important structural and chemical features in designing and developing new potent novel inhibitors for Corticotropin-releasing factor-1 receptor.

References

[1] B. P. Grone and K. P. Maruska, “A second corti-

cotropin-releasing hormone gene (CRH2) is conserved across vertebrate classes and expressed in the hindbrain of a basal neopterygian fish, the spotted gar", J. Comp. Neurol., Vol. 523, pp. 1125-1143, 2015.

[2] R. L. Hauger, D. E. Grigoriadis, M. F. Dallman, P. M. Plotsky, W. W. Vale, and F. M. Dautzenberg, "International union of pharmacology. XXXVI. Current status of the nomenclature for receptors for corticotropin-releasing factor and their ligands" Pharmacol. Rev., Vol. 55, pp. 21-26, 2003.

[3] N. Sato, K. Takagi, T. Suzuki, Y. Miki, S. Tanaka, S. Nagase, H. Warita, S. Fukudo, F. Sato, H. Sasano, and K. Ito, "Immunolocalization of corticotropin-releasing hormone (CRH) and its receptors (CRHR1 and CRHR2) in human endometrial carcinoma: CRHR1 as a potent prognostic factor", Int. J. Gynecol. Cancer, Vol. 24, pp. 1549-1557, 2014.

[4] F. Stamatelou, E. Deligeoroglou, N. Vrachnis, S. Iliodromiti, Z. Iliodromiti, S. Sifakis, G. Farmakides, and G. Creatsas, "Corticotropin-releasing hormone and progesterone plasma levels association with the onset and progression of labor", Clin. Exp. Obstet. Gyn., Vol. 40, pp. 568-571, 2013.

[5] F. C. Raadsheer, J. J. V. Heerikhuize, P. J. Lucassen, W. J. Hoogendijk, F. J. Tilders, and D. F. Swaab, "Corticotropin-releasing hormone mRNA levels in the paraventricular nucleus of patients with Alzheimer's disease and depression", Am. J. Psychiat., Vol. 152, pp. 1372-1376, 1995.

[6] H.-B. Fan, T. Zhang, K. Sun, S.-P. Song, S.-B. Cao, H.-L. Zhang, and W. Shen, "Corticotropin-releasing factor mediates bone cancer induced pain through neuronal activation in rat spinal cord", Tumor Biol., Vol. 36, pp. 9559-9565, 2015.

[7] V. Coric, H. H. Feldman, D. A. Oren, A. Shekhar, J. Pultz, R. C. Dockens, X. Wu, K. A. Gentile, S.-P. Huang, E. Emison, T. Delmonte, B. B. D'Souza, D. L. Zimbroff, J. A. Grebb, A. W. Goddard, and E. G. Stock, "Multicenter, randomized, double-blind, active comparator and placebo-controlled trial of a corticotropin-releasing factor receptor-1 antagonist in generalized anxiety disorder", Depress Anxiety, Vol. 27, pp. 417-425, 2010.

[8] E. M. Jutkiewicz, S. K. Wood, H. Houshyar, L.-W. Hsin, K. C. Rice, and J. H. Woods, "The effects of CRF antagonists, antalarmin, CP154, 526, LWH234, and R121919, in the forced swim test and on swim-induced increases in adrenocorticotropin in rats", Psychopharmacology, Vol. 180, pp. 215-223, 2005.

[9] B. Binneman, D. Feltner, S. Kolluri, Y. Shi, R. Qiu, and T. Stiger, "A 6-week randomized, placebo-controlled trial of CP-316,311 (a selective CRH1 antagonist) in the treatment of major depression", Am. J. Psychiat., Vol. 165, pp. 617-620, 2008.

[10] R. Pastor, C. S. Mckinnon, A. C. Scibelli, S. Burkhart-Kasch, C. Reed, A. E. Ryabinin, S. C. Coste, M. P. Stenzel-Poore, and T. J. Phillips, "Corticotropin-releasing factor-1 receptor involvement in behavioral neuroadaptation to ethanol: A urocortin1-independent mechanism", Proc. Natl. Acad. Sci. U.S.A., Vol. 105, pp. 9070-9075, 2008.

[11] K. Takedaa, T. Terauchi, M. Hashizume, K. Shikata, R. Taguchi, K. Murata-Tai, M. Fujisawa, Y. Takahashi, K. Shin, M. Ino, H. Shibata, and M. Yonaga, "Synthesis and structure–activity relationships of 8-substituted-2-aryl-5-alkylaminoquinolines: Potent, orally active corticotropin-releasing factor-1 receptor antagonists", Bioorgan. Med. Chem., Vol. 20, pp. 6559-6578, 2012.

[12] S. J. Cho and A. Tropsha, "Cross-validated R2-guided region selection for comparative molecular field analysis: A simple method to achieve consistent results", J. Med. Chem., Vol. 38, pp. 1060-1066, 1995.

[13] S. Wold, M. Sjöström, and L. Eriksson, "PLS-regression: a basic tool of chemometrics", Chemometr. Intell. Lab., Vol. 58, pp. 109-130, 2001.

[14] U. Debnath, S. Verma, S. Jain, S. B. Katti, and Y. S. Prabhakar, "Pyridones as NNRTIs against HIV-1 mutants: 3D-QSAR and protein informatics", J. Comput. Aid. Mol. Des., Vol. 27, pp. 637-654, 2013.

[15] D. Fernandez, J. Ortega-Castro, and J. Frau, "Human farnesyl pyrophosphate synthase inhibition by nitrogen bisphosphonates: A 3D-QSAR study", J. Comput. Aid. Mol. Des., Vol. 27, pp. 739-754, 2013.

[16] N. Santhosh Kumar and M. Thirumurthy, "3D-QSAR studies of 8-substituted-2-aryl-5-alkylaminoquinolines as Corticotropin-releasing factor-1 receptor antagonists." J. Chosun Natural Sci., Vol. 8, pp. 176-183, 2015.